J Mol Model (2010) 16:1039–1045
DOI 10.1007/s00894-009-0616-9

ORIGINAL PAPER

Binding of arachidonic acid and two flavonoid inhibitors to human 12- and 15-lipoxygenases: a steered molecular dynamics study

Carolina Mascayano · Gabriel Núñez · Waldo Acevedo · Marcos Caroli Rezende

Received: 11 August 2009 / Accepted: 7 October 2009 / Published online: 13 November 2009

Abstract The lipoxygenases (LOX) are a family of non-heme iron-containing dioxygenases which catalyze the stereospecific insertion of molecular oxygen into arachidonic acid, leading to hydroxy derivatives as end products. In this work, we docked arachidonic acid and two of its competitive inhibitors, flavonoids baicalein and quercetin, into the binding pockets of human 12- and 15-lipoxygenase. Steered molecular dynamics (SMD) simulations were employed to study the unbinding processes of the substrate and inhibitors from the two isoforms.

Keywords Arachidonic acid · Baicalein · Lipoxygenases · Quercetin · Steered molecular dynamics

Introduction

Lipoxygenases (LOX) are iron-containing enzymes that are responsible for the stereospecific dioxygenation of arachidonic acid. They are classified according to the position of dioxygenation of that substrate as 5-, 8-, 12- and 15-LOX. This important family of enzymes is involved with different human pathologies such as various forms of cancer (5-hLOX, 12-hLOX) [1], atherosclerosis (15-hLOX) [2], asthma (5-hLOX) [3] and psoriasis (12-hLOX) [4].

Steered molecular dynamics (SMD) simulations have been increasingly used to unravel the details of binding and unbinding of a biomolecule to a protein [5]. By applying an external force to a ligand, its unbinding from a protein is mimicked. Analyses of the dissociation pathway yields valuable information about the interactions between the protein and the biomolecule and the energetics of the binding process.

In a recent publication, the activity and selectivity of a number of 12- and 15-hLOX flavonoid inhibitors have been described and related with some structural features of these compounds [6]. These results prompted us to study in more details the interactions of two competitive flavonoid hLOX inhibitors with the active sites of these two lipoxygenase isoforms, with the aid of steered molecular dynamics.

In the present report we modeled two isoforms of human lipoxygenases, 12- and 15-hLOX, and docked arachidonic acid **1** and two flavonoid inhibitors, baicalein **2** and quercetin **3** [7], into their binding site. The unbinding process of these three molecules from the two isoenzymes was then investigated with the aid of SMD simulations (Fig. 1).

Methods

The sequences of human 12- and 15-LOX were obtained from the Pubmed database [8], the protein modeling employed the automated homology modeling program Modeller [9]. The 3D model was based on the refined crystal structure of rabbit reticulocyte 15-LOX (PDB entry code: 1LOX [10]), with 2.4 Å resolution, being refined with NAMD 2.6 [11], and validated by PROCHECK [12], PROSAII [13] and the ANOLEA web server [14].

Structures of arachidonic acid, quercetin and baicalein were built with the InsightII software [15]. Restraint electrostatic potential (RESP) charges were obtained at the B3LYP/6-31G** level of theory, employing the Gaussian 03 package [16].

C. Mascayano (✉) · G. Núñez · W. Acevedo · M. C. Rezende
Faculty of Chemistry and Biology,
University of Santiago of Chile,
Santiago, Chile
e-mail: carolina.mascayano@usach.cl

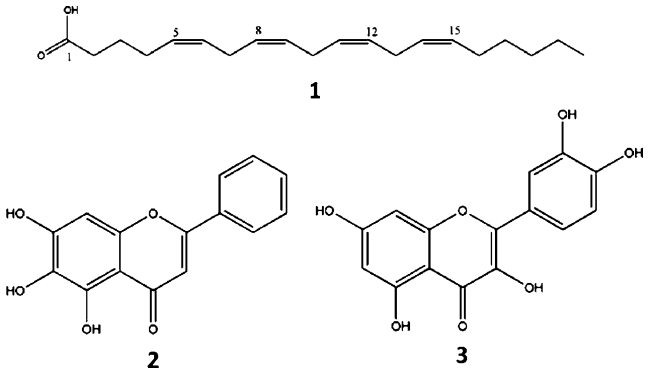

Fig. 1 Structures of arachidonic acid (**1**) and flavonoids baicalein (**2**) and quercetin (**3**)

Docking of substrate and flavonoids into the active site of the modeled 12- and 15-hLOX was performed with the AutoDock4 package [17], using a Lamarckian algorithm and assuming total flexibility of the inhibitors and partial flexibility of the HIS residues coordinated to Fe^{+3} inside the binding site. The grid maps were made up of 60×60×60 points, with a grid-point spacing of 0.375 Å. The AutoTors option was used to define the ligand torsions, and the docking results were then analyzed by a ranked cluster analysis, resulting in conformations with the highest overall binding energy (largest negative $-\Delta G_B$ value).

The SMD simulations were performed using NAMD 2.6 [11] with the Charmm33b force field [18]. The modeled enzyme with the docked substrate or inhibitor were soaked into a water box of 100×80×100 $Å^3$. The enzyme structure was thus surrounded by an aqueous layer at least 15-Å thick. A general protocol was followed, employing a cutoff value of 10 Å, and comprising an initial phase of 250 ps for the system equilibration, followed by 10,000 steps of minimization and 50 ps of heating from the 0 K up to 300 K, before each SMD simulation.

Steered molecular dynamics simulations of all equilibrated systems spanned 1.2 ns. The substrate or inhibitor was pulled out of the binding pocket at a constant speed of 0.0015 Å/ps by application of a variable external force to its center of mass. Each simulation was repeated 5 times. All graphical analyses were performed using the VMD software [19].

Results and discussion

Models of human 12- and 15-LOX were built by homology from the refined structures by Choi et al. of rabbit reticulocite 15-rLOX [10].

We next docked arachidonic acid into the active site of the two isoforms. Our results were in agreement with recent reports of homology modeling and docking studies of the same substrate inside the active site of 12- and 15-hLOX [20]. Some salient interactions inside the cavity are highlighted in Fig. 2. The central Fe^{+3} cation is coordinated by four histidine fragments (544, 360, 540 and 365) and one Ile663 in 15-hLOX. In 12-LOX, the His544 fragment is replaced by Asn544. The arachidonic chain approaches the central iron cation in the form of a loop, with the carboxylic group held at one end by electrostatic interactions with the amino groups of Arg402 and Gln406, in the case of 12-hLOX, or of Arg402 only, in the case of 15-hLOX. The other chain end interacts hydrophobically with Phe414. A comparison of the substrate conformations in the active site of the two isoforms sheds light on their specificity. In 12-LOX the iron cation is closer to the Δ^{11} double bond than in 15-LOX; in the latter, it is the Δ^{14} double bond that is closer to the metal cation (Fig. 2a and b).

CMD and SMD simulations of arachidonic acid

Starting from the docked conformation of arachidonic acid, conventional molecular dynamics (CMD) simulations were carried out, in order to equilibrate the substrate within the binding pocket of both isoenzymes. After 50 ps, the temperature and total energy of the system had attained a constant value, with fluctuations smaller than 5%. The main chain root-mean-square deviations (RMSD) from the starting structure of arachidonic acid also reached stable values (*ca.* 0.1) after 250 ps. At this point the SMD simulations were started. The arachidonic molecule was pulled out of the binding pocket of the enzyme by the application of an external force for 1.2 ns (Fig. 3a and b). The figures show graphs with the variation of the pulling force, in pN, with the simulation time, for 12- and 15-hLOX. Force peaks along the unbinding pathways are indications of stable interactions between the substrate and the enzyme, which are being disrupted as the substrate is being pulled out.

The force profiles for both isoforms are similar. Their analyses reveal different phases for the unbinding processes. Snapshots illustrating these processes are shown (Fig. 4). After equilibration inside the binding pocket, the arachidonic chain gradually unravels itself, with the carboxylic group leading the way toward the pocket entrance. As it passes between Gln406 and Arg402, the interactions of its carboxylic group with the amino groups of the two basic fragments are gradually disrupted, leading to a peak at 142 ps (snapshot a). It is then attracted toward the entrance by two lysine fragment, Lys179 and Lys157 (peak at 233 ps, snapshot b). Interaction with the former is stronger: as it is disrupted (peak at 322 ps, snapshot c), the carboxylic group crosses the pocket entrance and emerges into the aqueous bulk solution. The unfolded arachidonic chain follows it, passing through the entrance, and being completely surrounded by water molecules after 650 ps (snapshot d)

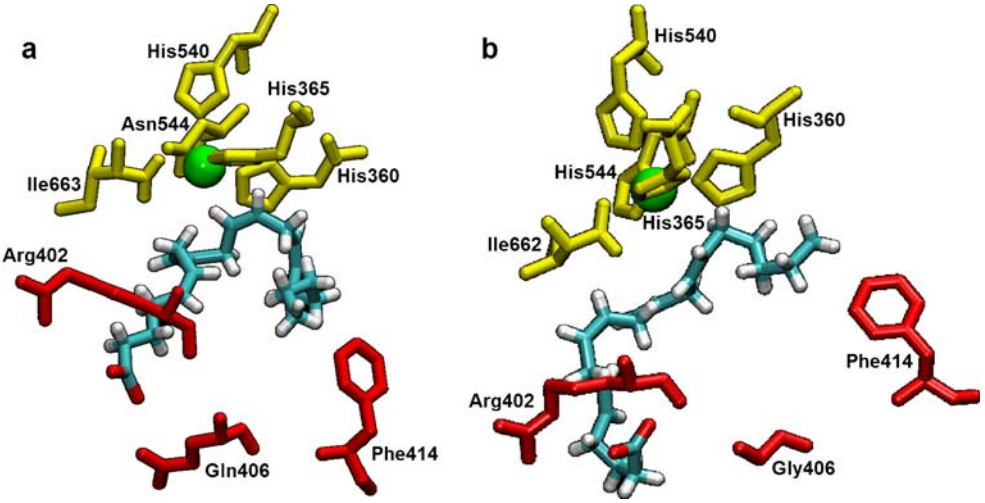

Fig. 2 Coordination spheres of arachidonic acid within the active sites of 12- (**a**) and 15-human lipoxygenase (**b**)

The starting point for the unbinding process of arachidonic acid from 15-hLOX differs from that of 12-hLOX by the absence of one basic fragment (Gln406) in 15-hLOX, capable of interaction with the carboxylic group. As a consequence, the disrupture of the carboxylic group from Arg402 that occurs at 150 ps (snapshot e) requires a pulling force of *ca.* 650 pN, a smaller value than that required for the analogous process in 12-hLOX (*ca*. 1000 pN). A second difference here is the absence of basic fragments lining the pocket entrance. The carboxylic group gradually breaks loose from the strong interactions with Arg402, leaving the enzyme and plunging into the bulk aqueous medium after 300 ps (snapshot f). The unfolded arachidonic chain follows it, and is completely pulled out of the enzyme into the aqueous solution after 450 ps.

A comparison of the force profiles (Fig. 3) may give us a clue as to the relative affinity of arachidonic acid for 12- and 15-hLOX. The greater number of stronger interactions with various fragments in 12-hLOX should lead to a larger value for the external work required to pull the substrate out of the enzyme pocket. This larger work value may be related with the free energy difference associated with the process [21] and ultimately with the greater affinity of arachidonic acid for the 12-hLOX isoform, in agreement with experimental observations [22].

CMD and SMD simulations of baicalein 2

Baicalein is a potent in vitro inhibitor of platelet 12-hLOX and of reticulocyte 15-hLOX [23]. Its mechanism of action is reductive, suggesting a direct binding of its catecholic moiety to iron. Although many authors have described it as a selective 12-hLOX inhibitor [6], steady-state inhibition kinetics have cast doubt on this assumption, yielding a small in vitro selectivity against 12-hLOX versus reticulocyte 15-hLOX. [23]

After docking baicalein into the active site of 15-hLOX and performing CMD simulations, we obtained a binding

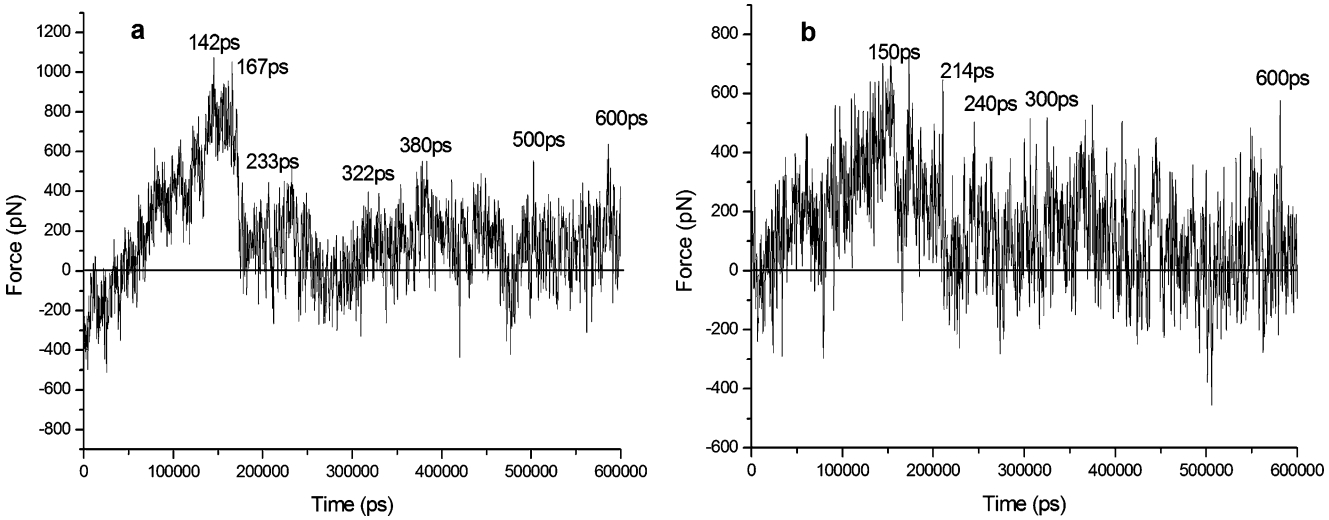

Fig. 3 Variation of the pulling force (in pN) exerted on arachidonic acid during its unbinding from 12- (**a**) and 15-hLOX (**b**) pockets

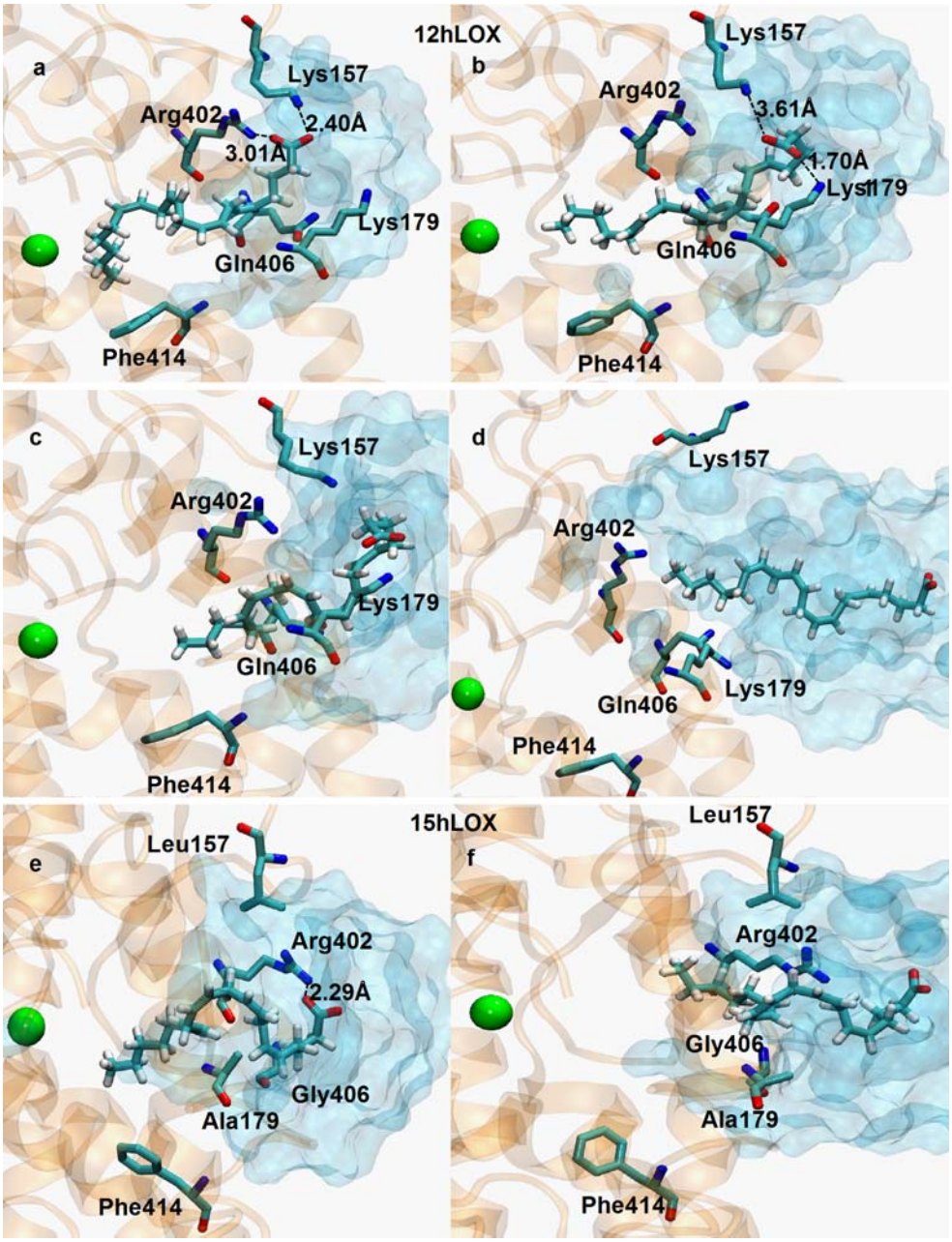

Fig. 4 Snapshots of the unbinding processes of arachidonic acid from the active sites of modeled 12-(**a**,**b**,**c** and **d**) and 15-hLOX(**e** and **f**)

mode that was in agreement with the pose obtained by Holman et al. [23], when baicalein was docked into the reticulocyte 15-hLOX. Starting from this pose, the obtained force graph for the unbinding process of baicalein from 15-hLOX (Fig. 5).

In snapshots (Fig. 6) corresponding to the main peaks of the force graph describe the main interactions of the inhibitor with some aminoacidic fragments, as it unbinds from the enzyme pocket.

Snapshot 6a reproduces the starting pose of the unbinding process. Baicalein binds to the iron atom through the catecholic 5- and deprotonated 6-OH groups. It is also held in place by a hydrogen bond (1.54 Å) between the 7-OH substituent and the carboxylic group of Glu356. The first peak at 375 ps corresponds to the breakage of the bond with iron (snapshot b). As the inhibitor turns away from the central metal, it finally breaks loose from Glu356 at 708 ps, heading toward the enzyme entrance into the aqueous phase (snapshot c)

CMD and SMD simulations of quercetin 3

Like baicalein **2**, quercetin **3** is reported to inhibit 12- and 15-LOX with significant IC_{50} values [24]. It is also assumed to bind to the iron center by a variety of modes, since it possesses five hydroxyl groups. We studied the

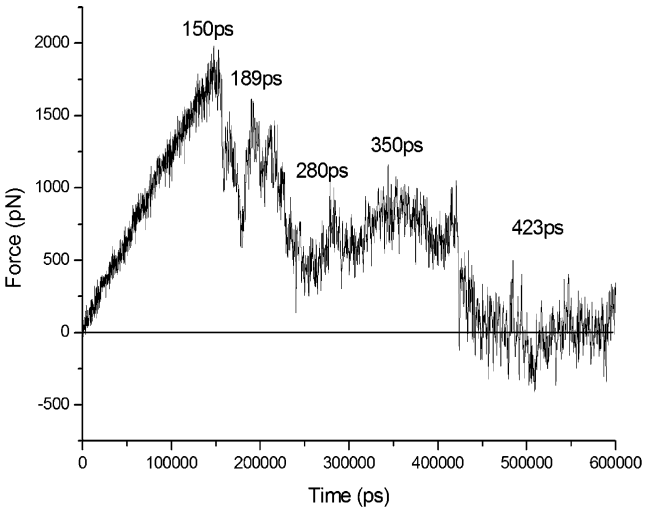

Fig. 5 Variation of the pulling force (in pN) exerted on baicalein during its unbinding from the 15-hLOX pocket

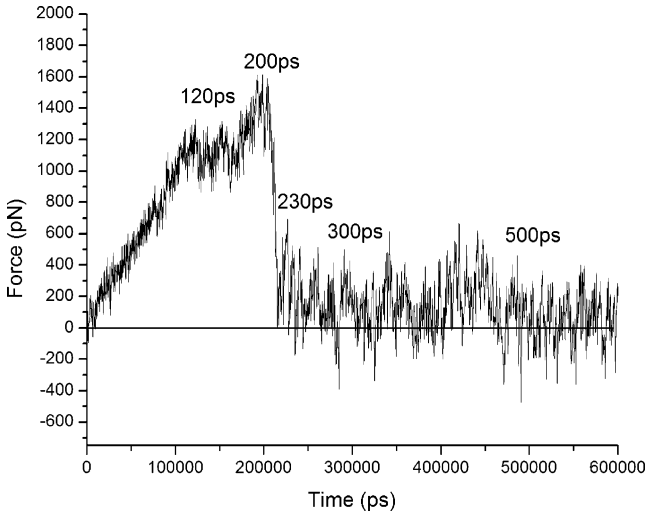

Fig. 7 Variation of the pulling force (in pN) exerted on quercetin during its unbinding from the 12-hLOX pocket

unbinding process of quercetin from 12-hLOX, following the same protocol described for baicalein (Fig. 7) shows the force graph for this unbinding process.

Unlike the graph obtained for baicalein, the variation of the pulling force with time for quercetin points to several interactions of the molecule with various aminoacidic fragments in the enzyme pocket.

These interactions are illustrated with snapshots, (Fig. 8) as the inhibitor gradually unbinds from the enzyme. After docking and a CMD simulation, the most stable pose, shown in snapshot a, corresponded to a binding mode to the iron through the deprotonated 3-OH group. Our result was in agreement with the 3-OH binding mode described by Antonczak et al. [24] in a study of the binding mode of quercetin to lipoxygenase-3. Interactions of the ring C catecholic groups of quercetin with Arg402 and Gln406 are also shown in the figure (snapshot a). These fragments still interact with the inhibitor, as it unbinds from the iron center at 120 ps (snapshot b). At 200 ps the interaction of the catecholic OH groups of ring C with Gln406 is disrupted, as this hydrophilic moiety orients itself toward the entrance (snapshot c). New interactions between Gln406 and the 3- and 5-OH groups are formed and disrupted at 230 and 300 ps (snapshots d and e) as the quercetin molecule finally emerges into the aqueous bulk solution.

The analysis of the unbinding processes of baicalein and quercetin from the LOX isoforms may help us interpret the differences in affinity of these two inhibitors. Quercetin is a much more effective inhibitor of 12-hLOX (IC_{50}= 0.44 μM) than baicalein of 15-hLOX (IC_{50}=9.11 μM) [6]. Two aspects of the unbinding processes depicted in Figs. 6 and 8 may be used to rationalize this difference: firstly, the transfer of the inhibitor molecule from the aqueous bulk solution to the enzyme pocket, and secondly, the stabilizing interactions of the inhibitors with amino-acidic fragments within the active site of the enzymes.

A comparison of snapshots 6c and 8d reveals that, as quercetin emerges into the aqueous solution, both its rings

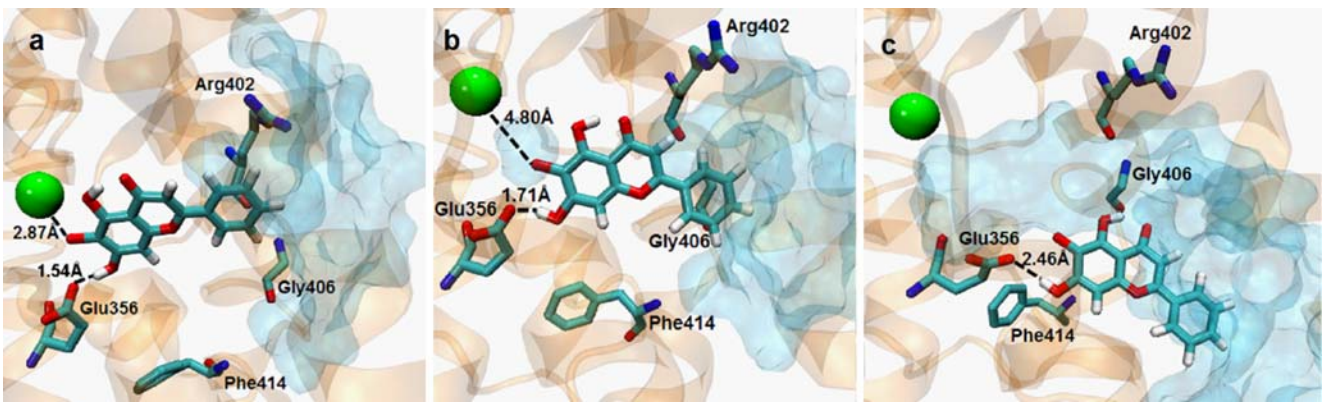

Fig. 6 Snapshots of the unbinding processes of baicalein from the active site of modeled 15-hLOX

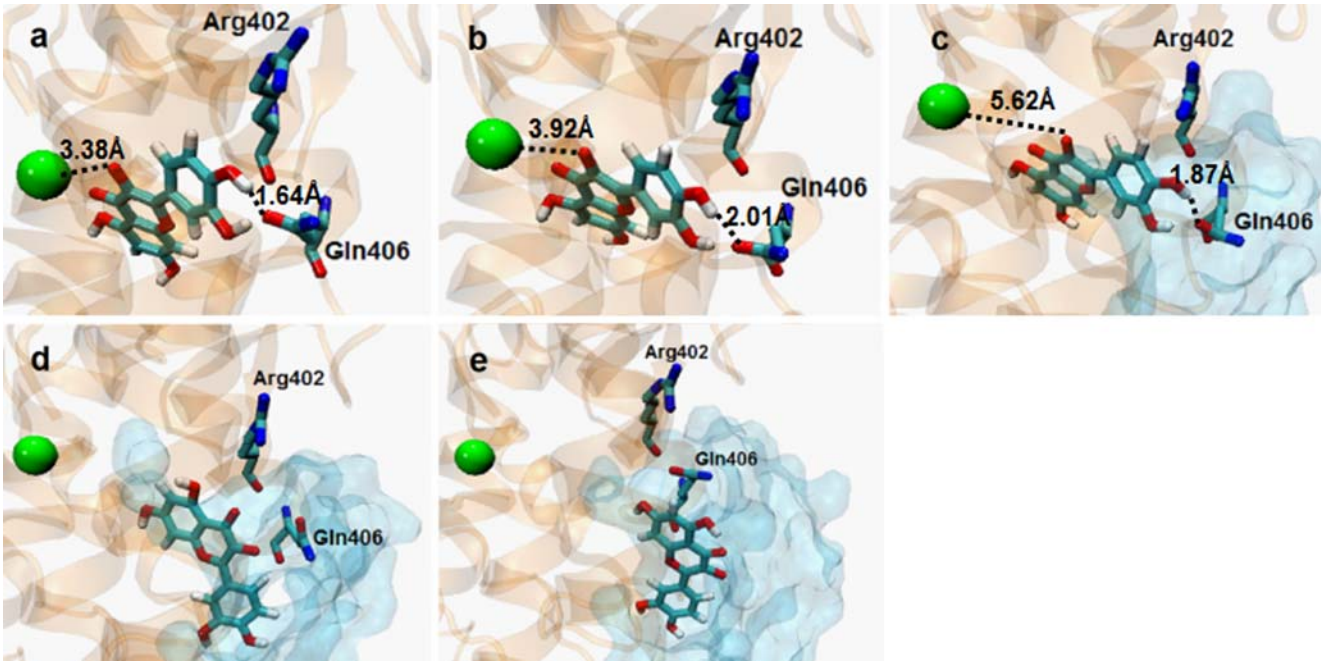

Fig. 8 Snapshots of the unbinding processes of quercetin from the binding pocket of modeled 12-hLOX

B and C are solvated by water; baicalein has only ring C available for solvation by water molecules. Transfer of the inhibitor molecules from the aqueous medium to the more hydrophobic enzyme pocket requires desolvation of the water molecules. In the case of baicalein, a total desolvation must take place, since rings A and C lead the inhibitor's penetration into the enzyme cavity (snapshot 6c). In the case of quercetin, only a partial desolvation is required: as the desolvated ring A penetrates the cavity, ring B is still surrounded by water molecules (snapshot 8d). The former process is therefore less favorable than the latter, leading to a greater affinity of quercetin for the LOX isoform.

Inside the active site of the enzyme, the inhibitors are stabilized by interactions with the iron cation and with aminoacidic fragments. In the case of baicalein, a hydrogen-bond interaction of its phenolic ring A with Glu356 helps stabilize the molecule (snapshot 6a). In the case of quercetin, the interactions with two basic amino-acids, Arg402 and Gln406 become as important as the binding force with the iron center (snapshot 8a). The increased importance of the two aminoacidic fragments in the latter case, when compared with only one fragment for baicalein, is seen in the force profiles (Figs. 5 and 7). For baicalein, unbinding from the iron of 15-hLOX at 150 ps requires a larger force than subsequent unbinding from Glu356 at 189 ps. In the case of quercetin, this situation is reversed, and unbinding from the two aminoacidic fragments at 200 ps demands a larger force than bond breakage from the iron center at 120 ps. Thus the contribution of two aminoacids in the binding of **3** within the active site of 12-hLOX, compared with only one fragment for binding **2** in 15-hLOX, increases the affinity of quercetin, in agreement with the reported IC_{50} values.

Conclusions

In conclusion, steered molecular dynamics were used to shed light on the binding processes of arachidonic acid into the active site of 12- and 15-hLOX. On its way toward the pocket entrance and into the aqueous bulk solution, the substrate interacts with Gln406, Arg402, Lys179, and Lys157 in 12-hLOX. By contrast, many of these interactions are absent in 15-hLOX, leading to a larger required work to pull the acid substrate out of the 12-hLOX pocket. This difference in overall binding energies may possibly explain the greater affinity of arachidonic acid for this isoform, in agreement with experimental values.

SMD techniques were also employed in the study of the dynamic interaction of two flavonoid inhibitors with 12- and 15-hLOX. Starting form binding modes that reproduced docking results from the literature [23, 24], the unbinding processes of baicalein **2** in 15-hLOX and quercetin **3** in 12-hLOX were studied. In the former case, the most important interactions of the inhibitor **2** in the enzyme pocket were with the iron center and with Glu356; in the latter case, interactions were mainly with the iron center and with Gln406 and Arg402. The latter interactions provide an additional stability to the binding mode of quercetin in 12-hLOX, leading to a greater affinity of this

flavonoid for this isoform. This is in agreement with experimental data [6].

Acknowledgments Financial support from FONDECYT project # 11075047 is gratefully acknowledged

References

1. Steele VE, Holmes CA, Hawk ET, Kopelovich L, Lubet RA, Crowell JA, Sigman CC, Kelloff GJ (1999) Lipoxygenase inhibitors as potential cancer chemopreventives. Cancer Epidemiol Biomark Prev 8:467–483
2. Ylä-Herttuala S, Rosenfeld ME, Parthasarathy S, Sigal E, Särkioja T, Witztum JL, Steinberg D (1991) Gene expression in macrophage-rich human atherosclerotic lesions.15-Lipoxygenase and acetyl low density lipoprotein receptor messenger RNA colocalize with oxidation specific lipid-protein adducts. J Clin Invest 87:1146–1152
3. Chu S, Tang L, Watney E, Chi EY, Henderson WR Jr (2000) In situ amplification of 5-Lipoxygenase and 5-Lipoxygenase-activating protein in allergic airway inflammation and inhibition by leukotriene blockade. J Immunol 165:4640–4648
4. Ikai K (1999) Psoriasis and the arachidonic acid cascade. J Dermatol Sci 21:135–146
5. Shen L, Shen J, Jiang H (2003) Steered molecular dynamic simulation on the binding of NNRTI to HIV-1 RT. Biophys J 84:3547–3563
6. Vasquez-Martinez Y, Ohri RV, Kenyon V, Holman TR, Sepúlveda-Boza S (2007) Structure-activity relationship studies of flavonoids as potent inhibitors of human platelet 12-hLO, reticulocyte 15-hLO-1, and prostate epithelial 15-hLO-2. Bioorg Med Chem 15:7408–7425
7. Sadik CD, Sies H, Schewe T (2003) Inhibition of 15-lipoxygenases by flavonoids: structure-activity relations and mode of action. Biochem Pharmacol 65:773–781
8. http://www.ncbi.nlm.nih.gov/pubmed/
9. Sali A, Blundell TL (1993) Comparative protein modelling by satisfaction of spatial restraints. J Mol Biol 234:779–815
10. Choi J, Chong JK, Kim S, Shin W (2007) Conformational flexibility in mammalian 15 S-lipoxygenase: reinterpretation of the crystallographic data. Proteins 70:1023–1032
11. Kale L, Skeel R, Bhandarkar M, Brunner R, Gursoy A, Krawetz N, Phillips J, Shinozaki A, Varadarajan K, Schulten K (1999) J Comput Phys 151:283–312
12. Laskowski RA, MacArthur MW, Moss DS, Thornton JM (1993) PROCHECK: a program to check the stereochemical quality of protein structures. J Appl Cryst 26:283–291
13. Sippl MJ (1993) Recognition of errors in three-dimensional structures of proteins. Proteins 17:355–362
14. Melo F, Devos D, Depiereux E, Feytmans E (1997) *ANOLEA*: a www server to assess protein structures. Intell Syst Mol Bio 91:110–113
15. Programs InsightII (1998) User Guide. Accelrys, San Diego
16. Pigache A, Cieplak P, Dupradeau FY (2004) Automatic and highly reproducible RESP and ESP charge derivation: Application to the development of programs RED and X RED. 227th ACS National Meeting, Anaheim, CA, USA
17. Morris GM, Goodsell DS, Halliday RS, Huey R, Hart WE, Belew RK, Olson AJ (1998) Automated docking using a Lamarckian genetic algorithm and an empirical binding free energy function. J Comput Chem 19:1639–1662
18. Brooks BR, Bruccoleri RE, Olafson BD, States DJ, Swaminathan S, Karplus M (1983) CHARMM: a program for macromolecular energy, minimization, and dynamics calculations. J Comput Chem 4:187–217
19. Humphrey W, Dalke A, Schulten K (1996) VMD - Visual Molecular Dynamics. J Mol Graphics 14:33–38
20. Wecksler AT, Kenyon V, Deschamps JD, Holman TR (2009) Substrate specificity changes for human reticulocyte and epithelial 15-lipoxygenases reveal allosteric product regulation. Biochemistry 28:7364–7375
21. Park S, Shulten K (2004) Calculating potentials of mean force fron steered molecular dynamics simulations. J Chem Phys 120:5946–5961
22. Wecksler AT, Jacquot C, Van der Donk WA, Holman TR (2009) Mechanistic investigations of human reticulocyte 15- and platelet 12-lipoxygenasees with arachidonic acid. Biochemistry 48:6259–6267
23. Deschamps JD, Kenyon VA, Holman TR (2006) Baicalein is a potent in vitro inhibitor against both reticulocyte 15-human and platelet 12-human lipoxygenase. Bioorg Med Chem 14:4295–4301
24. Fiorucci S, Golebiowski J, Cabrol-Bass D, Antonczak S (2008) Molecular simulations enlighten the binding mode of quercetin to lipoxygenase-3. Proteins 73:290–298